Antiferromagnetic resonances and magnetization of a canted antiferromagnet

A.A. Mukhin,[a] M. Biberacher,[b] A. Pimenov,[b,*] and A. Loidl[b]

[a] *General Physics Institute of the Russian Academy of Sciences, 119991 Moscow, Russia*
[b] *Experimentalphysik V, Elektronische Korrelationen und Magnetismus, Institut für Physik, Universität Augsburg, 86135 Augsburg, Germany*

1. Introduction

Physical properties of doped manganites remain the subject of intensive investigations. Initiated by the observation of colossal magnetoresistance [1] at the metal-to-insulator transition, the research efforts have been extended to the properties of different phases ranging from a ferromagnetic (FM) metal to an antiferromagnetic (AFM) insulator.

Among the topics still under debates is the low-doping part of the complex phase diagram of manganites [2]. The parent compounds, like $LaMnO_3$ or $CaMnO_3$ reveal antiferromagnetically ordered magnetic structure at low temperatures. Sr or Ca-doped $LaMnO_3$ with doping levels slightly larger than $\sim10\%$ becomes ferromagnetic insulators. Two possible scenarios can be imagined for the intermediate doping region between FM and AFM configurations. The first one is strongly favored theoretically [3] and assumes a phase separation into pure ferro- and antiferromagnetic regions with a doping-dependent volume ratio. The second scenario is based on a canted magnetic structure and corresponds to classical description of a doped antiferromagnet. The latter model was applied to the manganites already by de Gennes [4]. A recent discussion of this problem can be found in [5].

Magnetic resonances depend upon the local configuration of the magnetic moments and therefore provide important microscopic information about the magnetic structure on the atomic length scale. In this paper we analyze the consequences of the canted magnetic structure for the magnetic field-dependence of the antiferromagnetic resonances. We include new terms in the free energy in order to take into account the latest developments in the physics of manganites. On the basis of the presented model additional properties of the system can be calculated like field-dependent magnetization along different crystallographic directions.

2. Model of a canted structure

The model of a canted structure assumes the existence of two magnetic sublattices $(\vec{M}_1, \vec{M}_2)$ which are not exactly antiparallel, but oriented under an angle $\theta < 180°$.

* Corresponding author. Fax: +49-821-5983649.
E-mail address: Andrei.Pimenov@Physik.Uni-Augsburg.De (A. Pimenov).

As a working example, lightly Sr- or Ca-doped orthorhombic LaMnO$_3$ (space group Pbnm) can be considered. A canted A-type antiferromagnetic structure has been found in these compounds by neutron scattering [6]. A model similar to presented here has been applied to the manganites by de Gennes [4]. To account for the experimental data on manganites, an anisotropic contribution [7], as well as the contribution of the Dzyaloshinsky–Moria (DM) exchange [7,8] to the free energy were taken into account. With these additional terms the free energy of the system at zero temperature can be written as:

$$F(\vec{m}, \vec{l}) = \overbrace{\frac{1}{2}A\vec{m}^2}^{(1)} - \overbrace{B|\vec{m}|}^{(2)} + \overbrace{\frac{1}{2}K_x(m_x^2 + l_x^2) + \frac{1}{2}K_z(m_z^2 + l_z^2)}^{(3)}$$
$$- \underbrace{d_1 m_z l_y - d_2 m_y l_z}_{(4)} - \underbrace{M_0 \vec{m}\vec{H}}_{(5)}. \qquad (1)$$

In Eq. (1), $\vec{m}$ and $\vec{l}$ are dimensionless ferro- and antiferromagnetic vectors, which are defined as $\vec{m} = (\vec{M}_1 + \vec{M}_2)/2M_0$, $\vec{l} = (\vec{M}_1 - \vec{M}_2)/2M_0$ and satisfy the conditions

$$\vec{m}\vec{l} = 0, \qquad \vec{m}^2 + \vec{l}^2 = 1 \qquad (2)$$

since the sublattices $\vec{M}_1$ and $\vec{M}_2$ are assumed to be saturated at $T = 0$, and $M_0 = |\vec{M}_1| = |\vec{M}_2|$ is the saturation magnetization of the sublattices. Eq. (1) can be divided into five main contributions (indicated in Eq. (1)), which will be described below.

- *Antiferromagnetic exchange (1)*. It accounts for the antiferromagnetic coupling of the ferromagnetic planes due to the super-exchange interaction $J_{ij}\vec{S}_i\vec{S}_j$. The exchange constant A is given by the super-exchange integral along the c-axis $J_\parallel$: $A = -2NzJ_\parallel S^2$, where N is the number of the magnetic ions and $z = 2$ is the number of the nearest Mn neighbors along c.
- *Double exchange (2)*. The double exchange [9] is a competing interaction to the (1) and causes a FM coupling between the Mn ions due to strong dependence of the transfer energy t_{ij} of e_g electrons(holes) on a respective orientation θ_{ij} of neighboring Mn spins $\vec{S}_i$ and $\vec{S}_j$: $t_{ij} = t_{\parallel,\perp}\cos(\theta_{ij}/2) = t_{\parallel,\perp} \mid \vec{S}_i - \vec{S}_j \mid /2S$, where $t_{\parallel,\perp}$ are the transfer integrals along and perpendicular to the c-axis, respectively. In the two-sublattice approximation the angle-dependent part of this interaction is reduced to the second term of Eq. (1) with a constant $B = xNzt_\parallel/2$, where x is the concentration of the holes, i.e., Mn^{4+}-ions in doped manganite.
- *Anisotropy energy (3) and DM-interaction (4)*. The anisotropic terms result from the single-ion anisotropy determined by the crystal field (CF) acting on Mn^{3+} ions $DS_{\zeta i}^2 + E(S_{\xi i}^2 - S_{\eta i}^2)$, where $S_{\xi i}, S_{\eta i}, S_{\zeta i}$ are the spin components in the local axes of Mn^{3+} related to the Mn–O bonds of the MnO$_6$ octahedra, and

from the antisymmetric Dzyaloshinsky–Moriya exchange $\Sigma_{i,j}\vec{d}_{ij}[\vec{S}_i\vec{S}_j]$. The contributions of these interactions to $K_{x,z}$ and $d_{1,2}$ are determined both by the parameters of the CF and DM Hamiltonians as well as an orientation of their local axes with respect to the crystallographic ones, implying a dependence on the crystal distortions [10,11]. These interactions lead to $K_{x,z} > 0$ and a stabilization of the A$_y$F$_z$ configuration in lightly doped LaMnO$_3$. Here A$_y$F$_z$ indicates AFM-order along y (crystallographic b-axis) and FM-order along z (crystallographic c-axis). In general, a contribution to a weak ferromagnetic moment is determined both by the DM-exchange ($d_- = d_1 - d_2 \neq 0$) and the single-ion anisotropy ($d_+ = d_1 + d_2 \neq 0$).

- *External magnetic field (5)*. The contribution of the external field to the free energy is determined by the corresponding g-factors of Mn^{3+} and Mn^{4+} ions, which are, in general, slightly anisotropic. Neglecting this anisotropy and assuming $g = 2$, the corresponding Zeeman interaction can be expressed via the saturation magnetization, which in a case of doped manganites is given by: $M_0 = (1-x)M_0(\text{Mn}^{3+}) + xM_0(\text{Mn}^{4+}) = 4\mu_\text{B} \cdot (1-x) + 3\mu_\text{B} \cdot x$.

The equilibrium arrangement of the sublattices can be obtained minimizing the free energy given by Eq. (1): $\frac{\partial F}{\partial \vec{m}} = \frac{\partial F}{\partial \vec{l}} = 0$. The frequencies of the resonance modes are calculated in the limit of small perturbations from the equations of motion

$$\begin{cases} \frac{M_0}{\gamma}\dot{\vec{m}} = \left[\vec{m} \times \frac{\partial \vec{F}}{\partial \vec{m}}\right] + \left[\vec{l} \times \frac{\partial \vec{F}}{\partial \vec{l}}\right] \\ \frac{M_0}{\gamma}\dot{\vec{l}} = \left[\vec{m} \times \frac{\partial \vec{F}}{\partial \vec{l}}\right] + \left[\vec{l} \times \frac{\partial \vec{F}}{\partial \vec{m}}\right] \end{cases}, \qquad (3)$$

where $\gamma = 2\mu_\text{B}/\hbar$ is the gyromagnetic ratio.

In the limit of small perturbations ($\vec{m} = \vec{m}_0 + \Delta\vec{m}$ and $\vec{l} = \vec{l}_0 + \Delta\vec{l}$) the linearized equations of motion take the form:

$$\begin{cases} \frac{M_0}{\gamma}\Delta\dot{\vec{m}} = \left[\Delta\vec{m} \times \vec{F}_m^0\right] + \left[\vec{m}_0 \times \Delta\vec{F}_m\right] + \left[\Delta\vec{l} \times \vec{F}_l^0\right] + \left[\vec{l}_0 \times \Delta\vec{F}_l\right] \\ \frac{M_0}{\gamma}\Delta\dot{\vec{l}} = \left[\Delta\vec{m} \times \vec{F}_l^0\right] + \left[\vec{m}_0 \times \Delta\vec{F}_l\right] + \left[\Delta\vec{l} \times \vec{F}_m^0\right] + \left[\vec{l}_0 \times \Delta\vec{F}_m\right] \end{cases}, \qquad (4)$$

where the following definitions have been applied:

$$\vec{F}_m^0 \equiv \frac{\partial \vec{F}}{\partial \vec{m}^0}, \quad \vec{F}_l^0 \equiv \frac{\partial \vec{F}}{\partial \vec{l}^0},$$

$$\Delta\vec{F}_m \equiv \Delta\vec{m}\frac{\partial \vec{F}}{\partial \vec{m}^0 \partial \vec{m}^0} + \Delta\vec{l}\frac{\partial \vec{F}}{\partial \vec{m}^0 \partial \vec{l}^0} + \Delta\vec{H}\frac{\partial \vec{F}}{\partial \vec{m}^0 \partial \vec{H}^0}, \quad \text{and}$$

$$\Delta\vec{F}_l \equiv \Delta\vec{m}\frac{\partial \vec{F}}{\partial \vec{l}^0 \partial \vec{m}^0} + \Delta\vec{l}\frac{\partial \vec{F}}{\partial \vec{l}^0 \partial \vec{l}^0} + \Delta\vec{H}\frac{\partial \vec{F}}{\partial \vec{l}^0 \partial \vec{H}^0}.$$

The superscript "0" indicates the static equilibrium value of the variables. Solving Eq. (4) the magnetic field dependence of the AFMR (antiferromagnetic

resonance) modes can be obtained. In the following the solution will be presented for the external magnetic field along the main crystallographic directions.

2.1. External magnetic field along the c-axis

In the geometry $H\|c$ the solution for the AFMR-modes takes the most simple form. In this case the equilibrium coordinates of the magnetic vectors contain one component only: $\vec{m}_0 = (0, 0, m_z^0)$; $\vec{l}_0 = (0, l_y^0, 0)$. To simplify the expressions, we omit the index "0" and denote m and l to be the equilibrium values of the ferro- and antiferromagnetic vectors (see Fig. 1).

Separation of Eq. (4) into scalar equations for the spatial coordinates (x, y, z) leads to six scalar equations. However, for a geometry $H\|c$ these equations can be separated into two independent groups, which therefore represent two independent antiferromagnetic modes. The first group involves the components (Δm_x, Δm_y, and Δl_z) and the corresponding mode can be termed a ferromagnetic-like mode, the F-mode:

$$\begin{cases} \frac{M_0}{\gamma}\Delta\dot{m}_x = \Delta m_y F_{m,z}^0 - \Delta l_z F_{l,y}^0 - m_z \Delta F_{m,y} + l_y \Delta F_{l,z}, \\ \frac{M_0}{\gamma}\Delta\dot{m}_y = -\Delta m_x F_{m,z}^0 + m_z \Delta F_{m,x}, \\ \frac{M_0}{\gamma}\Delta\dot{l}_z = \Delta m_x F_{l,y}^0 - l_y \Delta F_{m,x}. \end{cases} \quad (5)$$

The second group of the linearized equations of motion includes (Δm_z, Δl_x, and Δl_y) and describes the behavior of the AF-mode:

$$\begin{cases} \frac{M_0}{\gamma}\Delta\dot{m}_z = \Delta l_x F_{l,y}^0 - l_y \Delta F_{l,x}, \\ \frac{M_0}{\gamma}\Delta\dot{l}_x = -\Delta m_z F_{l,y}^0 - m_z \Delta F_{l,y} + \Delta l_y F_{m,z}^0 + l_y \Delta F_{m,z}, \\ \frac{M_0}{\gamma}\Delta\dot{l}_y = m_z \Delta F_{l,x} - \Delta l_x F_{m,z}^0. \end{cases} \quad (6)$$

From the normalization conditions for the vectors $\vec{l}$ and $\vec{m}$ (Eq. (2)) the following relations follow: $\Delta l_y = -\Delta m_z \frac{m_z}{l_y}$ and $\Delta l_z = -\Delta m_y \frac{l_y}{m_z}$. Therefore, each set of equations for F- and AF-modes contains two independent equations, only. Searching for the harmonic ($\Delta m, \Delta l \propto e^{-i\omega t}$) solution the following equations for the resonance frequencies are obtained:
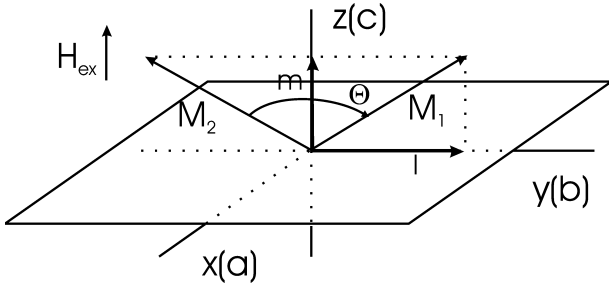F-mode:

Fig. 1. Geometry of the magnetic sublattices for external field parallel to the c-axis.

$$\begin{vmatrix} i\omega & K_z(m_z^2 - l_y^2)/m_z - M_0 H_z - 2d_+ l_y \\ m_z(K_x - K_z) + d_1 l_y + M_0 H_z & i\omega \end{vmatrix} = 0 \quad (7)$$

AF-mode:

$$\begin{vmatrix} i\omega & -(d_1 m_z + K_x l_y) \\ l_y(A + K_z) + d_1 m_z(3 + m_z^2/l_y^2) & i\omega \end{vmatrix} = 0, \quad (8)$$

where $d_+ = d_1 + d_2$. Here we used the equality $F_{m_z}^0 = \frac{m_z}{l_y}F_{l_y}^0$ which follows from the equilibrium conditions. We further recall that $m_z = \cos\frac{\theta}{2}$ and $l_y = \sin\frac{\theta}{2}$, where the angle between the sublattice magnetizations had been obtained from the minimum of the free energy:

$$\cos\frac{\theta}{2} = \frac{B + M_0 H_z + d_1 \sin\frac{\theta}{2}}{A + K_z + d_1 \cot\frac{\theta}{2}}. \quad (9)$$

Now the solution for the frequencies of both AFMR modes can be written explicitly:

$$\frac{M_0^2}{\gamma^2}\omega_F^2 = \left[M_0 H_z \cos\frac{\theta}{2} + d_+ \sin\theta - K_z \cos\theta\right] \cdot \left[d_1 \sin\frac{\theta}{2} + M_0 H_z + (K_x - K_z)\cos\frac{\theta}{2}\right] \bigg/ \cos\frac{\theta}{2}, \quad (10)$$

$$\frac{M_0^2}{\gamma^2}\omega_{AF}^2 = \left[K_x \sin\frac{\theta}{2} + d_1 \cos\frac{\theta}{2}\right] \cdot \left[(A + K_z)\sin\frac{\theta}{2} + \left(3 + \cot^2\frac{\theta_0}{2}\right)\cdot d_1 \cos\frac{\theta}{2}\right]. \quad (11)$$

Two modes can be separated into oscillations of the ferro- and antiferromagnetic vectors and are shown in Fig. 2. The AFMR-modes can therefore be termed quasi-ferromagnetic (F-mode) and quasi-antiferromagnetic (AF-mode) resonances. The interaction of the modes with the electromagnetic field is realized via the term $(M_0\vec{m}\cdot\vec{H})$ in the free energy, Eq. (1). The oscillations in the F-mode involve the following components of the magnetic vectors: $\mathbf{m}_a$, $\mathbf{m}_b$, and $\mathbf{l}_c$ (Fig. 2, left panel). This mode can therefore be excited by the electromagnetic wave with the ac-magnetic field ($\tilde{h}$) having a nonzero component in the ab-plane. By analogy, the AF-mode (Fig. 2, right panel), which involves ($\mathbf{m}_c$, $\mathbf{l}_a$, $\mathbf{l}_b$) is excited for ($\tilde{h}$) parallel to the c-axis [12].

2.2. External magnetic field along the a-axis

For external magnetic fields along the a-axis, the canted spin-configuration is additionally tilted in the x-direction as shown in Fig. 3. The equilibrium coordinates of the magnetic vectors read now:
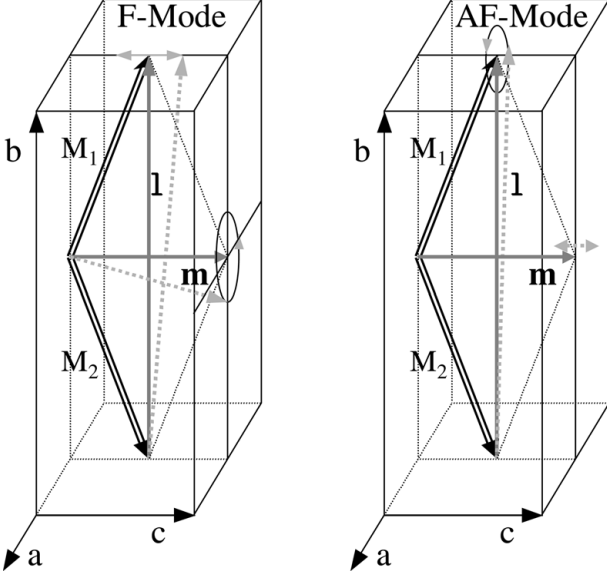
Fig. 2. Antiferromagnetic modes of a canted antiferromagnet. The magnetic moments of the two sublattices $\vec{M}_1$ and $\vec{M}_2$ correspond to adjacent ab-layers in lightly doped LaMnO$_3$ and are brought to the same point for simplicity. $\mathbf{m} = (\vec{M}_1 + \vec{M}_2)/2M_0$, ferromagnetic moment; $\mathbf{l} = (\vec{M}_1 - \vec{M}_2)/2M_0$, antiferromagnetic moment. The oscillations corresponding to two possible modes are also shown (ellipses and double arrows). The quasi-ferromagnetic mode (F) is excited by $\tilde{h}\|a$ and $\tilde{h}\|b$, the quasi-antiferromagnetic mode (AF) by $\tilde{h}\|c$.
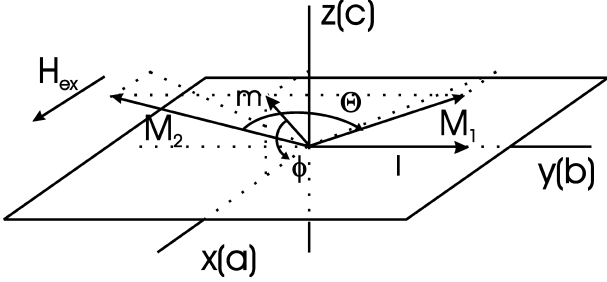

Fig. 3. Orientation of the magnetic sublattices in the external field parallel to the a-axis.

$$\vec{m} = (m_x, 0, m_z) \equiv \left(\cos\frac{\theta}{2}\cos\varphi, 0, \cos\frac{\theta}{2}\sin\varphi \right);$$

$$\vec{l} = (0, l_y, 0) \equiv \left(0, \sin\frac{\theta}{2}, 0 \right).$$

The equilibrium values of the angle θ and φ are obtained in analogy to the previous subsection solving the equations:

$$(K_z - K_x)\cos\frac{\theta}{2}\cos\varphi\sin\varphi + M_0 H \sin\varphi - d_1 \sin\frac{\theta}{2}\cos\varphi$$
$$= 0, \quad \text{and} \tag{12}$$

$$-\frac{1}{2}[A + K_x \cos\varphi^2 + K_z \sin\varphi^2]\sin\theta + [B + M_0 H \cos\varphi]$$
$$\times \sin\frac{\theta}{2} - d_1 \sin\varphi\cos\theta = 0. \tag{13}$$

Two antiferromagnetic modes cannot be separated in this case and are therefore coupled. A procedure, similar to that of the previous section, leads finally to the following equation for the resonance frequencies:

$$\begin{vmatrix} i\omega & 0 & D_{13} & D_{14} \\ 0 & i\omega & D_{23} & D_{24} \\ D_{31} & D_{32} & i\omega & 0 \\ D_{41} & D_{42} & 0 & i\omega \end{vmatrix} = 0. \tag{14}$$

Here the elements of the matrix in Eq. (14) are given by

$$D_{13} = -K_z \frac{l_y^2 - m_z^2}{m_z} - 2d_+ l_y,$$

$$D_{14} = -K_z \frac{m_x l_y}{m_z} - d_+ m_x,$$

$$D_{23} = M_0 H_x - K_x m_x - d_2 \frac{m_x l_y}{m_z},$$

$$D_{24} = -l_y K_x - \frac{d_1 m_z^2 + d_2 m_x^2}{m_z},$$

$$D_{31} = (K_x - K_z)m_z + d_1 \frac{l_y^2 - m_x^2}{l_y},$$

$$D_{32} = (K_x - K_z)m_x - M_0 H_x - d_1 \frac{m_x m_z}{l_y},$$

$$D_{41} = -\frac{m_x}{l_y}\left[\left(A + K_z - \frac{B}{m^3} \right)m_z - 2d_1 l_y \right],$$

$$D_{42} = l_y\left(A + K_z - B\frac{m_x^2}{m^3} \right) + d_1 m_z \ \ 3 + \frac{m_z^2}{l_y^2}.$$

Eq. (14) leads to two possible resonance frequencies:

$$-\left(\frac{M_0}{\gamma}\omega_{1,2} \right)^2 = E \pm \sqrt{E^2 + Q}, \quad \text{with} \tag{15}$$

$$E = \frac{1}{2}(D_{13}D_{31} + D_{23}D_{32} + D_{42}D_{24} + D_{14}D_{41}), \quad \text{and}$$

$$Q = D_{42}D_{31}D_{23}D_{14} + D_{41}D_{13}D_{24}D_{32}$$
$$- D_{42}D_{24}D_{13}D_{31} - D_{41}D_{14}D_{32}D_{23}.$$

2.3. External magnetic field along the b-axis

The external magnetic field parallel to the b-axis leads to the rotation of the magnetic moments in the bc-plane by an angle ϕ (Fig. 4). In high magnetic fields a spin–flop transition takes place within this geometry, i.e., the magnetic moments rotate by $\phi = \pi/2$ from the field-free position. In this case the ferromagnetic vector $\vec{m}$ is oriented along the b-axis after the transition.

The equilibrium position of the magnetic vectors $\vec{m}_0 = (0, m_y, m_z) \equiv (0, \cos\frac{\theta}{2}\sin\phi, \cos\frac{\theta}{2}\cos\phi)$; $\vec{l}_0 = (0, l_y, l_z) \equiv (0, \sin\frac{\theta}{2}\cos\phi, -\sin\frac{\theta}{2}\sin\phi)$ in low fields, i.e., below a
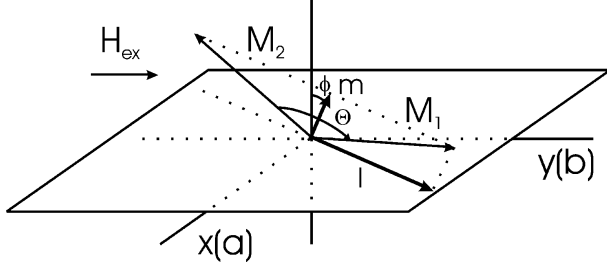
Fig. 4. Orientation of the magnetic sublattices in the external field parallel to the *b*-axis.

threshold field of the spin–reorientation (spin–flop) transition, is determined by the set of equations

$$(M_0 H)^2 \left[K_z \cos\frac{\theta}{2} + d_+ \sin\frac{\theta}{2} \right]$$
$$= [K_z \cos\theta - d_+ \sin\theta]^2 \cdot \left[(A + K_z) \cos\frac{\theta}{2} + \frac{d_1 \cos\theta}{\sin\frac{\theta}{2}} - B \right], \tag{16}$$

$$\sin\phi = \frac{M_0 H \cos\frac{\theta}{2}}{K_z \cos\theta + d_+ \sin\theta}. \tag{17}$$

Above the threshold field, i.e., in the state $\phi = \pi/2$ ($m \| b$), the angle θ is calculated from

$$M_0 H = (A - K_z) \cos\frac{\theta}{2} - \frac{d_2 \cos\theta}{\sin\frac{\theta}{2}} - B. \tag{18}$$

The threshold field, above which this state is stable, is determined from Eq. (16) with the critical value of the angle θ given by:

$$\left(A + K_z - d_2 \cot\frac{\theta}{2} \right) \cos^2\frac{\theta}{2} - \left(B - d_2 \sin\frac{\theta}{2} \right) \cos\frac{\theta}{2} - K_z$$
$$- d_+ \sin\theta = 0 \tag{19}$$

As in the case $\vec{H} \| a$ the antiferromagnetic modes cannot be separated. The resonance frequencies are determined by

$$\begin{vmatrix} i\omega & D_{12} & D_{13} & 0 \\ D_{21} & i\omega & 0 & D_{24} \\ D_{31} & 0 & i\omega & D_{34} \\ 0 & D_{42} & D_{43} & i\omega \end{vmatrix} = 0, \tag{20}$$

Here the elements of the matrix in Eq. (20) are given by

$$D_{12} = M_0 H_y + K_z(m_y + \alpha_1 l_y + \alpha_3 l_z) + d_+(l_z + \alpha_1 m_z + \alpha_3 m_y),$$
$$D_{13} = K_z(m_z - \alpha_1 l_z + \alpha_2 l_y) - d_+(l_y - \alpha_1 m_y - \alpha_2 m_z),$$
$$D_{21} = -d_2 l_z - K_x m_y - M_0 H_y,$$
$$D_{24} = -d_1 m_z - K_x l_y,$$
$$D_{31} = (K_x - K_z) m_z + d_1 l_y,$$
$$D_{34} = (K_x - K_z) l_z + d_2 m_y,$$
$$D_{42} = (A + K_z) l_y - B\frac{m_y}{m^3}(m_z l_z + m_y l_y) + \alpha_1 K_z(m_y + l_z(\alpha_2 - \alpha_3))$$
$$+ d_1[m_z(2 + \alpha_1^2 + \alpha_3^2) - \alpha_3 l_y] - \alpha_1 d_2[l_z + (\alpha_3 - \alpha_2) m_y],$$

$$D_{43} = -A l_z + B\frac{m_z}{m^3}(m_z l_z + m_y l_y) + K_z(l_z(1 + \alpha_1^2 + \alpha_2^2) + \alpha_2 m_y)$$
$$- d_2[(2 + \alpha_1^2 + \alpha_2^2) m_y - \alpha_2 l_z] + \alpha_1 d_1[l_y + (\alpha_2 - \alpha_3) m_z],$$

with the parameters $\alpha_{1,2,3}$ defined as

$$\alpha_1 = \frac{m_z m_y - l_z l_y}{m_y l_z - m_z l_y}; \quad \alpha_2 = \frac{m_y^2 - l_y^2}{m_y l_z - m_z l_y};$$
$$\alpha_3 = \frac{l_z^2 - m_z^2}{m_y l_z - m_z l_y};$$

These equations remain valid above the spin–flop transition as well, with the angle θ obtained from Eq. (18) and with $\phi = \pi/2$. Eq. (20) finally leads to the solution for resonance frequencies

$$-\left(\frac{M_0}{\gamma} \omega_{1,2} \right)^2 = E \pm \sqrt{E^2 + Q}, \quad \text{with} \tag{21}$$

$$E = \frac{1}{2}(D_{24}D_{42} + D_{34}D_{43} + D_{12}D_{21} + D_{31}D_{13}), \quad \text{and}$$
$$Q = D_{12}D_{31}D_{43}D_{24} + D_{13}D_{21}D_{34}D_{42} - D_{12}D_{21}D_{34}D_{43}$$
$$- D_{13}D_{31}D_{24}D_{42}.$$

Above the spin–flop transition field the modes become uncoupled and their frequencies read $-(\frac{M_0}{\gamma}\omega_F)^2 = D_{31}D_{13}$ and $-(\frac{M_0}{\gamma}\omega_{AF})^2 = D_{24}D_{42}$, similar to the case $H \| c$.

2.4. Discussion

To understand the physics of the problem, it is instructive to consider a limiting case of small canting angles. Assuming $(B, d_{1,2}, K_x, K_z, M_0 H) \ll A$, the approximate solution for the magnetization can be written as:

$$M_x \equiv M_0 m_x = \chi_\perp H_x(B + d_1)/d_1, \quad \vec{H} = (H_x, 0, 0), \tag{22}$$

$$M_y \equiv M_0 m_y = \chi_{\text{rot}} H_y, \quad \vec{H} = (0, H_y, 0), \tag{23}$$

$$M_z \equiv M_0 m_z = M_z^0 + \chi_\perp H_z, \quad \vec{H} = (0, 0, H_z). \tag{24}$$

where $M_z^0 \equiv M_s = M_0(B + d_1)/(A + K_z)$ is the spontaneous magnetic moment along the *c*-axis, $\chi_\perp = M_0^2/(A + K_z)$ and $\chi_{\text{rot}} = M_s^2/(K_z + 2d_+ M_s/M_0) \approx M_s^2/K_z$ are the transverse and rotational susceptibilities, respectively.

Within the same approximations the frequencies of the AFMR modes for $H \| c$ read:

$$\left(\frac{M_0}{\gamma} \omega_F \right)^2 = \left(\frac{M_0}{\gamma} \omega_F^0 \right)^2 + (d_1 + 2d_+)M_0 H_z + (M_0 H_z)^2, \tag{25}$$

$$\left(\frac{M_0}{\gamma} \omega_{AF} \right)^2 = \left(\frac{M_0}{\gamma} \omega_{AF}^0 \right)^2 + d_1 M_0 H_z, \tag{26}$$

where $\omega_{F,AF}^0$ are the frequencies at $\mathbf{H} = 0$

$$\left(\frac{M_0}{\gamma}\omega_F^0\right)^2 = AK_z\frac{d_1}{B+d_1} \qquad (27)$$

$$\left(\frac{M_0}{\gamma}\omega_{AF}^0\right)^2 = AK_x + d_1(d_1+B) \approx AK_x. \qquad (28)$$

The analysis of Eq. (24) shows that the z-axis exhibits weak ferromagnetism because the magnetization is non-zero in the absence of an external magnetic field. The magnetization along the y-axis (Eq. (23)) is determined by the small rotational susceptibility and disappears in the pure antiferromagnetic case ($B = d_1 = 0$). The low-field susceptibility along the x-direction (Eq. (22)) is enhanced compared to the susceptibility along the z-axis by the factor $(B + d_1)/d_1$. Qualitatively similar behavior of the magnetization is observed in Fig. 5 [14]. The solid lines in Fig. 5 were calculated using the field dependence of the magnetization angles Eqs. (9), (12), (13), (16), and (17) and describe the experimental data reasonably well. A small static moment along the y-axis is possibly due to a weak twinning of the sample. The absolute values of the parameters of the model were obtained by simultaneously fitting the magnetization curves and the values of the AFMR frequencies without external magnetic field ($v_F = 5.8\,\mathrm{cm}^{-1}$, $v_{AF} = 13.8\,\mathrm{cm}^{-1}$). Despite the relatively large number of parameters in Eq. (1) ($A, B, d_{1,2}, K_x, K_z$), the requirement of a simultaneous fit of magnetization and resonance frequencies leads to an unambiguous determination of the parameters: $A = 4.67 \times 10^7$ erg/g, $B = 7.4 \times 10^6$ erg/g, $K_z = 3.33 \times 10^6$ erg/g, $K_x = 3.42 \times 10^6$ erg/g, $d_1 = 2.1 \times 10^6$ erg/g, and $M_0 = 92.14$ emu/g. In these calculations we adopted that $d_2 \approx -d_1$. These parameters correspond to the average canting angle $180° - \theta = 22°$.

The presented two-sublattice model for manganites has been successfully applied to the doping dependence
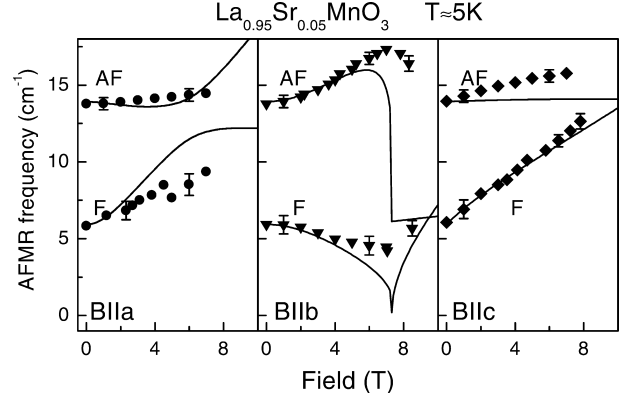
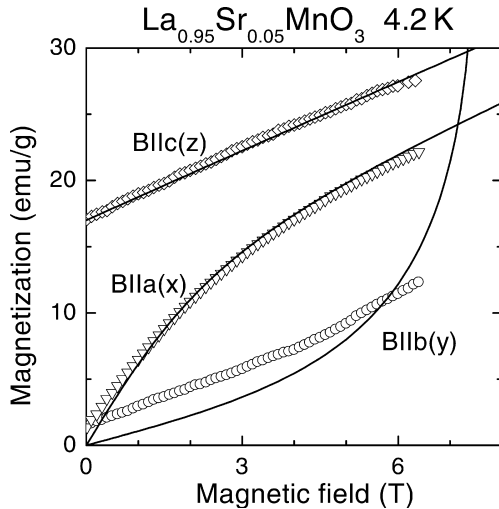Fig. 6. Magnetic field dependence of the AFMR frequencies in $La_{0.95}Sr_{0.05}MnO_3$ at low temperatures. Points, experiment [14]; lines, model calculations.

of the AFMR-modes in $La_{1-x}Sr_xMnO_3$ [13], and to the magnetic-field dependence of the resonances in untwinned $La_{0.95}Sr_{0.05}MnO_3$ [14]. The magnetic field dependencies of the resonance frequencies of both AFMR lines are shown in Fig. 6. The solid lines in Fig. 6 were calculated on the basis of the model discussed above. However, the parameters of the model *were already fixed* by fitting the magnetization curves and absolute values of the AFMR frequencies in the absence of magnetic field. Having this in mind, the theoretical curves describe the experimental data reasonably well. The most important feature of Fig. 6 is the softening of the FM-mode for $B\|b$. This softening represents a common property of magnetic resonance in antiferro-magnets and is followed by the field-induced rearrangement of the magnetic structure (spin–flop) at a critical value of magnetic field. The softening of the FM-mode at low fields is in good agreement with the model calculations. The behavior for higher fields ($B\sim7$T) deviates significantly from the model predictions. These deviations are most probably due to the extreme sensitivity of the data with respect to the exact orientation of the static magnetic field and the neglect of the higher-order terms in Eq. (1). The angular dependence of a critical behavior in a canted antiferromagnet has been calculated in details by Hagedorn and Gyorgy [15]. These calculations show that already a misalignment of the magnetic field as low as one degree strongly suppress the softening of the FM-line in the vicinity of the critical field. Most probably, similar effects explain the deviations observed in Fig. 6. In addition, we note that the AFMR modes obey the excitation conditions as described discussing Fig. 2.

Fig. 5. Magnetization of $La_{0.95}Sr_{0.05}MnO_3$ single crystal along different crystallographic axes at $T = 4.2$ K [14]. Symbols represent the experimental data, lines are calculated according to the presented model.

## 3. Conclusions

Two-sublattice model, which includes the double-exchange mechanism, have been applied to a canted

magnetic structure. The static magnetization and the AFMR resonance frequencies have been calculated for external magnetic field along the principal crystallographic axes. As a working example, the magnetization, positions and excitation conditions of the AFMR modes in $La_{0.95}Sr_{0.05}MnO_3$ single crystal have been calculated and compared to the experimental data.

References

[1] K. Chahara, T. Ohno, M. Kasai, Y. Kozono, Magnetoresistance in magnetic manganese oxide with intrinsic antiferromagnetic spin structure, Appl. Phys. Lett. 63 (1993) 1990–1992;
R. von Helmolt, J. Wecker, B. Holzapfel, L. Schulz, K. Samwer, Giant negative magnetoresistance in perovskitelike $La_{2/3}Ba_{1/3}MnO_x$ ferromagnetic films, Phys. Rev. Lett. 71 (1993) 2331–2333;
S. Jin, T.H. Tiefel, M. McCormack, R.A. Fastnacht, R. Ramesh, L.H. Chen, Thousandfold change in resistivity in magnetoresistive La-Ca-Mn-O films, Science 264 (1994) 413–415.

[2] M. Paraskevopoulos, F. Mayr, J. Hemberger, A. Loidl, R. Heichele, D. Maurer, V. Müller, A.A. Mukhin, A.M. Balbashov, Magnetic properties and the phase diagram of $La_{1-x}Sr_xMnO_3$ for $x \leqslant 0.2$, J. Phys.: Condens. Matter 12 (2000) 3993–4011.

[3] E.L. Nagaev, Lanthanum manganites and other giant-magneto-resistance magnetic conductors, Sov. Phys.-Uspekhi 39 (1996) 781–805;
E. Dagotto, T. Hotta, A. Moreo, Colossal magnetoresistant materials: the key role of phase separation, Phys. Rep. 344 (2001) 1–153;
M.Yu. Kagan, K.I. Kugel', Inhomogeneous charge distributions and phase separation in manganites, Phys.-Uspekhi 44 (2001) 553–570.

[4] P.-G. de Gennes, Effects of double exchange in magnetic crystals, Phys. Rev. 118 (1960) 141–154.

[5] D. Ivannikov, M. Biberacher, H.-A. Krugvon Nidda, A. Pimenov, A. Loidl, A.A. Mukhin, A.M. Balbashov, High-field ESR on the spin dynamics in $La_{1-x}Sr_xMnO_3$ ($x \leqslant 0.175$), Phys. Rev. B 65 (2002) 214422.

[6] M. Hennion, F. Moussa, G. Biotteau, J. Rodríguez-Carvajal, L. Pinsard, A. Revcolevschi, Evidence of anisotropic magnetic polarons in $La_{0.94}Sr_{0.06}MnO_3$ by neutron scattering and comparison with Ca-doped manganites, Phys. Rev. B 61 (2000) 9513–9522;
G. Biotteau, M. Hennion, F. Moussa, J. Rodríguez-Carvajal, L. Pinsard, A. Revcolevschi, Y.M. Mukovskii, D. Shulyatev, Approach to the metal-insulator transition in $La_{1-x}Ca_xMnO_3$ ($0 \leqslant x \leqslant 0.2$): Magnetic inhomogeneity and spin-wave anomaly, Phys. Rev. B 64 (2001) 104421.

[7] T. Morya, Weak ferromagnetism, in: G.T. Rado, H. Suhl (Eds.), Magnetism, vol. I, Academic Press, New York, 1984.

[8] I. Dzyaloshinsky, A thermodynamic theory of weak ferromagnetism of antiferromagnetics, J. Phys. Chem. Sol. 4 (1958) 241–255.

[9] C. Zener, Interaction between the d-shells in the transition metals. II. Ferromagnetic compounds of manganese with perovskite structure, Phys. Rev. 82 (1951) 403–405.

[10] J. Deisenhofer, M.V. Eremin, D.V. Zakharov, V.A. Ivanshin, R.M. Eremina, H.-A. Krug von Nidda, A.A. Mukhin, M. Balbashov, A. Loidl, Crystal field, Dzyaloshinsky–Moriya interaction, and orbital order in $La_{0.95}Sr_{0.05}MnO_3$ probed by ESR, Phys. Rev. B 65 (2002) 104440; cond-mat/0108515 (unpublished).

[11] L.E. Gonchar, A.E. Nikiforov, S.E. Popov, Interplay between orbital, charge and magnetic orderings in $R_{1-x}A_xMnO_3$ ($x = 0, 0.5$), J. Magn. Magn. Mater. 223 (2001) 175–191;
L.E. Gonchar, A.E. Nikiforov, S.E. Popov, Antiferromagnetic resonance spectrum in $LaMnO_3$: interrelation of the orbital structure and the magnetic properties, J. Exp. Theor. Phys. 91 (2000) 1221–1229.

[12] G.F. Herrmann, Resonance and high frequency susceptibility in canted antiferromagnetic substances, J. Phys. Chem. Sol. 24 (1963) 597–606;
G.F. Herrmann, Magnetic resonances and susceptibility in orthoferrites, Phys. Rev. 133 (1964) A1334–A1344.

[13] A.A. Mukhin, V.Yu. Ivanov, V.D. Travkin, A. Pimenov, A. Loidl, A.M. Balbashov, Antiferromagnetic resonance in the canted phase of $La_{1-x}Sr_xMnO_3$: experimental evidence against electronic phase separation, Europhys. Lett. 49 (2000) 514–520.

[14] A. Pimenov, M. Biberacher, D. Ivannikov, A. Loidl, V.Yu. Ivanov, A.A. Mukhin, A.M. Balbashov, High-field antiferromagnetic resonance in single-crystalline $La_{0.05}Sr_{0.95}MnO_3$: experimental evidence for the existence of a canted magnetic structure, Phys. Rev. B 62 (2000) 5685–5689.

[15] F.B. Hagedorn, E.M. Gyorgy, Complex susceptibility and resonance frequencies of canted antiferromagnets, Phys. Rev. 174 (1968) 540–545.